Time-lapse full-waveform inversion with uncertainty quantification

Zijun Deng, Rafael Orozco, Abhinav Prakash Gahlot, Felix J. Herrmann, Georgia Institute of Technology*

SUMMARY

Carbon Capture, Utilization, and Storage (CCUS) is one of the few technologies capable of achieving net-negative CO_2 emissions to mitigate climate change. It also supports net-zero CO_2 operations in applications such as Enhanced Oil Recovery (EOR). However, accurately predicting fluid flow patterns in reservoirs remains challenging due to inherent uncertainties in CO_2 plume dynamics and reservoir properties. Previous deterministic seismic imaging methods, such as the Joint Recovery Method (JRM), have provided valuable insights including ending reliance on replication of the surveys to get good repeatability of the surveys, but lack the capability to communicate uncertainty, thus limiting their utility for risk-informed decision-making in monitoring. To overcome this limitation, we introduce the Probabilistic JRM (πJRM), which computes wave-equation based posterior distributions for each monitoring survey while leveraging a shared generative model. By explicitly quantifying uncertainties, πJRM enhances risk assessment capabilities and supports decision-making in CCUS applications.

INTRODUCTION

Effective risk mitigation in subsurface energy storage relies on probabilistic frameworks to quantify uncertainties and optimize decision-making. This is critical for applications such as conventional hydrocarbon extraction, hydrogen storage, enhanced oil recovery (EOR), and carbon capture, utilization, and storage (CCUS)—a suite of technologies that enable large-scale energy storage and contribute to reducing atmospheric CO_2 concentrations. Monitoring time-lapse changes in the subsurface is essential for assessing reservoir performance, detecting potential leakage pathways, and tracking the evolution of injected fluids (Ringrose, 2020). However, these processes are inherently uncertain due to spatial and temporal variability in reservoir properties such as permeability, porosity, and caprock integrity (Ringrose, 2023). Consequently, advanced monitoring techniques, coupled with rigorous uncertainty quantification, are necessary to improve subsurface characterization, mitigate operational risks, and support data-driven decision-making in energy storage and carbon management.

Seismic imaging has emerged as the primary monitoring technique for CCUS due to its ability to provide high-resolution images of subsurface structures (Lumley, 2001; Chadwick and Arts, 2010). Time-lapse seismic imaging, also known as 4D seismic monitoring, enables the tracking of CO_2 plume evolution over time by comparing seismic surveys acquired at different stages of injection. This method has been successfully applied in various CCUS projects (Arts et al., 2004; Wilson et al., 2004). Time-lapse imaging relies on wave-based inversion techniques, including full-waveform inversion (FWI) (Sun et al., 2024) and reverse-time migration (RTM) (Yin et al., 2021). Among these, FWI has gained significant attention due to its ability to reconstruct high-resolution velocity models. However, FWI remains computationally expensive, and, more importantly, the ill-posed nature of wave-based imaging makes it highly sensitive to noise and introduces significant uncertainties (Virieux and Operto, 2009). In CCUS applications, these challenges make it difficult to achieve reliable imaging results, particularly when monitoring small-scale CO_2 plume evolution.

The Joint Recovery Method (JRM) has been proposed as an approach incorporated with wave-based imaging to enhance time-lapse seismic imaging by leveraging the shared structure among multiple surveys (Oghenekohwo and Herrmann, 2015; Yin et al., 2021; Gahlot et al., 2023). JRM assumes that certain features of the subsurface remain unchanged between surveys, such as geological formations that are unaffected by multiphase fluid flow injection. By jointly inverting these shared features across multiple surveys, JRM improves the consistency and quality of time-lapse imaging compared to independent inversions of each survey. However, despite its advantages, JRM remains a deterministic approach and does not account for uncertainty introduced by ill-posedness, limiting its utility as a decision-support tool.

To overcome these limitations, we propose the Probabilistic Joint Recovery Method (πJRM), a novel approach that incorporates uncertainty estimation into the joint inversion framework. The πJRM computes the posterior distribution of subsurface properties, acoustic wavespeeds in our case, at each monitoring survey, leveraging the shared structure among surveys through a shared generative model (SGM), which captures shared structures among multiple surveys while maintaining flexibility in uncertainty modeling. This is achieved by integrating the Deep Decoder and latent space into the inversion framework, allowing for the representation of complex posterior distributions (Heckel and Hand, 2019). As a follow-up work of πJRM on post-stack inversion, we extend and validate our probabilistic framework on nonlinear FWI. By explicitly modeling uncertainty, πJRM provides probabilistic estimates of subsurface properties, enhancing the reliability of CO_2 monitoring and supporting risk-informed decision-making in CCUS projects.

We evaluate πJRM on synthetic experiments, highlighting its capability to reconstruct CO_2 plume evolution accurately and quantify uncertainty for improved monitoring decisions. Furthermore, we validate the hypothesis, previously established in deterministic joint recovery frameworks, that non-replicated acquisition strategies can improve time-lapse imaging results within our probabilistic setting. This approach addresses the practical challenges associated with the high costs and inefficiencies of replicated seismic surveys in CCUS monitoring. Overall, πJRM contributes to optimizing subsurface operations by providing robust insights across applications such as CO_2 storage assessment, reservoir management, and EOR.

METHODOLOGY

Inspired by previous work that leverages shared structure on reconstructing black holes (Leong et al., 2023), we adapted the idea to jointly solve N time-lapse inversion problems. Our approach takes N seismic measurements as input and produces N posterior distributions of the time-lapse surveys as output. To incorporate probabilistic modeling within the JRM framework, we design πJRM to employ a Shared Generative Model (SGM). The SGM is capable of extracting structural common components that remain invariant over time and inherently provides regularization by constraining the reconstructed surveys to lie within the range of the generator (Heckel and Hand, 2019). Meanwhile, unique features of each survey, defined as innovation components, are captured by assigning different latent distributions to the SGM for each monitoring survey.

Probabilistic Joint Recovery Model

Our goal is to recover the N posterior distributions for N time-lapse acoustic properties derived from N noisy time-lapse surveys. To demonstrate our framework in a clear manner, we illustrate the methodology using $N = 2$ time-lapse surveys, though the framework generalizes to $N \geq 2$. Mathematically, we jointly solve the two following forward models,

$$\mathscr{F}_1(\mathbf{x}_1^*) + \varepsilon_1 = \mathbf{y}_1 \text{ and } \mathscr{F}_2(\mathbf{x}_2^*) + \varepsilon_2 = \mathbf{y}_2.$$

Here, $\mathbf{x}_i^*$, where $i = 1,2$, denotes the ground-truth slowness of the subsurface, $\mathbf{y}_i$ denotes the noisy surveys obtained by applying nonlinear wave propagation operator $\mathscr{F}_i$ of FWI to $\mathbf{x}_i^*$ with noise ε_i. Note that each survey corresponds to 240 sources; for simplicity, we did not explicitly demonstrate the summation of data misfit over all the shot records in our objective function.

To integrate uncertainty, we model the solutions probabilistically by using an SGM, G_θ, which decodes latent distributions into the posterior estimates $\mathbf{x}_1$ and $\mathbf{x}_2$—i.e.,

$$\mathbf{x}_1 \sim G_\theta(q_{\phi_1}(\mathbf{z}_1)) \text{ and } \mathbf{x}_2 \sim G_\theta(q_{\phi_2}(\mathbf{z}_2)) \,,$$

where $\mathbf{z}_i \sim \mathscr{N}(0,I)$ is the standard Gaussian distribution, and q_{ϕ_i} represents the Gaussian mixture model (GMM) used to encode the different baseline and monitor(s) monitors. The objective function is then defined as:

$$\min_{\theta,\phi_1,\phi_2} \mathbb{E}_{\mathbf{z}_1\sim\mathscr{N}(0,I)}\left[\|\mathscr{F}_1(G_\theta(q_{\phi_1}(\mathbf{z}_1)) - \mathbf{y}_1\|_2^2\right] + \mathbb{E}_{\mathbf{z}_2\sim\mathscr{N}(0,I)}\left[\|\mathscr{F}_2(G_\theta(q_{\phi_2}(\mathbf{z}_2)) - \mathbf{y}_2\|_2^2\right]$$

which minimizes the summation of misfit between the forward-modeled time-lapse surveys and the observed time-lapse surveys with respect to the parameters θ of SGM and ϕ_i's of the GMMs. Finally, time-lapse images are generated by computing the differences between posterior means of $\mathbf{x}_1$ and $\mathbf{x}_2$ after each inference.

Probabilistic Independent Recovery Model

To quantify the performance improvement obtained by jointly versus independently solving N inverse problems, we introduce the Probabilistic Independent Recovery Model (pIRM) as a baseline comparison:

$$\min_{\theta_1,\phi_1} \mathbb{E}_{\mathbf{z}_1\sim\mathscr{N}(0,I)}\left[\|\mathscr{F}_1(G_{\theta_1}(q_{\phi_1}(\mathbf{z}_1))) - \mathbf{y}_1\|_2^2\right]$$
$$\text{and } \min_{\theta_2,\phi_2} \mathbb{E}_{\mathbf{z}_2\sim\mathscr{N}(0,I)}\left[\|\mathscr{F}_2(G_{\theta_2}(q_{\phi_2}(\mathbf{z}_2))) - \mathbf{y}_2\|_2^2\right].$$

In pIRM, separate SGM G_{θ_i} is trained independently for each seismic survey, i, while πJRM leverages a shared generative model that identifies common structural components across all surveys, thereby exploiting shared features to enhance reconstruction quality.

Weak formulation

When using the πJRM, the computational cost to evaluate the wave propagation operator and its gradient at each iteration is significant. To mitigate this, we adopt and extend the weak formulation introduced by Orozco et al. (2024), which decouples forward operator evaluations from network parameter updates in Algorithm 1. Specifically, forward operator evaluations and gradient calculations (lines 3) are performed in an outer loop, while updates of network parameters (lines 8-9) take place in an inner loop.

In this structure, to further take advantage of the shared structure across the time-lapse surveys, we incorporated nonlinear JRM (nJRM), a deterministic JRM that captures the full nonlinear relationship in the wave equation, within the iterative variable-update process. We explicitly decompose the model into a common component, $\mathbf{x}_0$, and innovation components, $\delta\mathbf{x}_i$, and solve them using the Projected Quasi-Newton (PQN) algorithm following nJRM. Note that the vectors $\mathbf{x}_0$ and $\delta\mathbf{x}_i$'s are updated accordingly based on the same gradient computed for $\delta\mathbf{x}_i$. A mathematical proof demonstrating the equivalence of these gradients is provided in Gahlot et al. (2023).

This decoupling significantly reduces computational costs by limiting forward operator evaluations to 30, a manageable number compared to the number of network parameter updates needed ($500000 \sim$), thereby achieving a more computationally viable optimization procedure.

Algorithm 1 Probabilistic Joint Recovery Model (πJRM) with Weak Formulation

1: **for** $ii = 1 : \text{maxiter}_1$ **do**
2: **for** $i = 1 : N$ **do**
3: $\mathbf{g}_i = \nabla_{\delta\mathbf{x}_i}\left[\frac{1}{2\sigma^2}\|\mathscr{F}_i(\mathbf{x}_0 + \delta\mathbf{x}_i) - \mathbf{y}_i\|_2^2\right]$
4: $\mathbf{x}_0 = \mathbf{x}_0 - \tau\mathbf{g}_i$
5: $\delta\mathbf{x}_i = \delta\mathbf{x}_i - \tau\mathbf{g}_i$
6: **end for**
7: **for** $iii = 1 : \text{maxiter}_2$ **do**
8: $\mathscr{L}(\phi_i,\theta) = \sum_{i=1}^N\left[\frac{1}{2\gamma^2}\|(\mathbf{x}_0 + \delta\mathbf{x}_i) - G_\theta\left(q_{\phi_i}(\mathbf{z}_i)\right)\|_2^2\right]$
9: $(\phi_i,\theta) \leftarrow \text{ADAM}(\mathscr{L}(\phi_i,\theta))$
10: **end for**
11: **end for**

SYNTHETIC CASE STUDY

We validate our method on synthetic velocity models representing a realistic 2D CCUS scenario with dimensions of 5.9 km ×

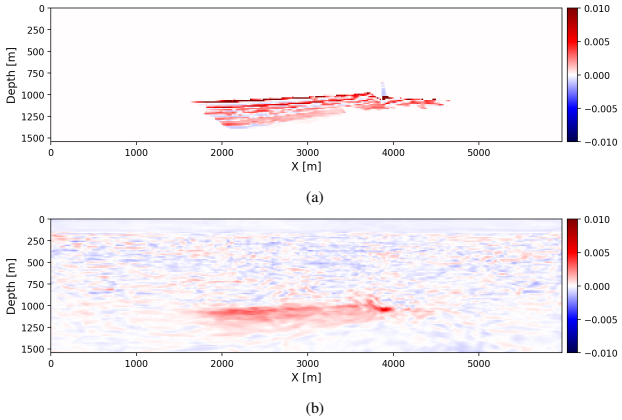

Figure 1: Comparison of time-lapse images. (a) Ground truth time-lapse difference $\mathbf{x}_2^* - \mathbf{x}_1^*$; (b) time-lapse image with πJRM for $N = 2$ surveys.

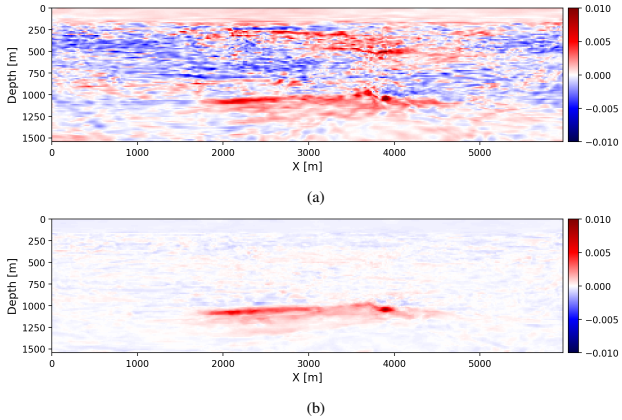

Figure 2: Comparison of time-lapse images. (a) Time-lapse image with pIRM for $N = 2$ surveys; (b) time-lapse image with πJRM for $N = 6$ surveys.

1.6 km, discretized into a grid of 398×103. We simulate CO_2 fluid flow at an injection site using the *JutulDarcy.jl* simulator (Møyner et al., 2023). The seismic acquisition setup consists of 240 seismic sources and 120 receivers. We model seismic wave propagation using a 14.5 Hz Ricker wavelet sampled at 2 ms intervals and performed FWI for time-lapse monitoring with the open-source software *JUDI.jl* (Witte et al., 2019). Additionally, to simulate realistic conditions, we introduce bandwidth-limited noise with a signal-to-noise ratio (SNR) of 10 dB to the seismic shot data. We update squared slowness ($[\mathrm{s/km}]^2$) for baseline and monitor surveys using nJRM, where each inversion uses the PQN algorithm from *SetIntersectionProjection.jl* (Peters and Herrmann, 2019), with box constraints added to the common components and the innovation components to restrict their range to 0 to 0.45 $[\mathrm{s/km}]^2$ and -0.05 to 0.05 $[\mathrm{s/km}]^2$, respectively. In addition, we add total variation constraints to encourage smoothness and consistency in the updated slowness model. Note that no explicit regularization is added during network training. The time-lapse reconstructions are obtained by calculating the differences between the posterior mean slowness derived from the inference in Figures 1, 2.

To evaluate the weak formulation algorithm, we perform tests using both two and six surveys. Specifically, we compute posterior means using 50 posterior samples from both baseline and the final monitoring surveys generated by the trained SGM. Results demonstrated in Figures 1, 2 clearly indicate that the πJRM significantly outperforms the pIRM. The time-lapse difference images from πJRM accurately retain the shape and structure of the true CO_2 plume, whereas pIRM results show significantly greater noise, particularly within regions of common structural features. Moreover, the six-survey configuration, representing more frequent acquisition intervals typical in CCUS projects, demonstrates better reconstruction quality. Figures 1b, 2b display enhanced detail, such as accurately showing higher values at plume boundaries and significantly reducing background noise compared to the two-survey scenario.

To quantify the uncertainty associated with our reconstructions, we calculate the standard deviation of posterior samples of the last vintage and the error compared to the ground truth time-lapse. Consistent with the time-lapse difference results, the uncertainty and error maps in Figures 4, 5 for pIRM, two-survey πJRM, and six-survey πJRM clearly illustrate the superiority of πJRM in reducing both errors and uncertainties. As expected, increasing the number of surveys within a given time period reduced uncertainty, as the SGM is capable of further leveraging shared structures across multiple surveys with more data collected. Overall, these results underscore πJRM's strength in effectively capturing and reducing uncertainty, thus significantly improving reconstruction accuracy compared to independently inverted surveys.

Non-replicated vs. replicated surveys

We hypothesize that non-replicated acquisition, where source locations differ across surveys, provides more information about the subsurface compared to replicated acquisition, where source locations remain fixed over time. This hypothesis has been previously validated within the deterministic JRM framework (Oghenekohwo and Herrmann, 2015; Yin et al., 2021; Gahlot et al., 2023), and here we aim to verify its benefits within πJRM. To test this hypothesis, we simulate non-replicated acquisition by randomly varying source locations across the different time-lapse surveys, while in the replicated scenario, we maintained consistent source locations throughout all time steps.

Figure 3 compares the results of replicated and non-replicated surveys, while the bottom plots in Figures 4 and 5 show the corresponding uncertainty and error distributions. From the error plots, we observe that the replicated survey exhibits a higher background noise level compared to the non-replicated case. For quantitative evaluation, we employ the metric Normalized Root Mean Square difference (NRMS). The NRMS value for both scenarios is close to 10%, indicating strong repeatability between baseline and monitoring surveys. The NRMS value for non-replicated acquisitions across six vintages is 9.5%, lower than that for replicated acquisitions, which

is 10.1%. These results confirm that the advantages of non-replicated survey designs are preserved in a probabilistic context. We therefore conclude that non-replicated acquisition strategies can enhance both the accuracy and cost-effectiveness of time-lapse imaging—an essential consideration for reliable and sustainable monitoring in CCUS operations.

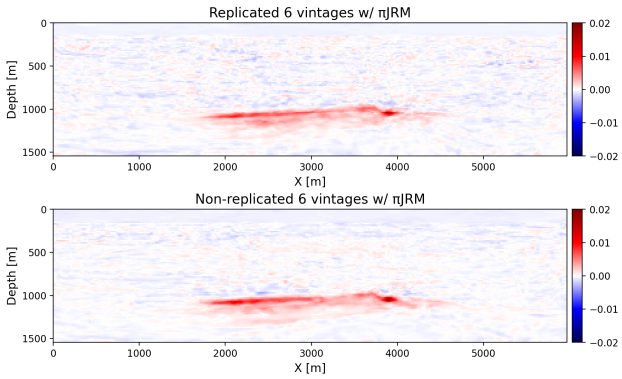

Figure 3: Comparison of time-lapse inversions with replicated (top) and non-replicated (bottom) acquisition.

CONCLUSIONS

In this work, we introduce a novel probabilistic approach to time-lapse monitoring, which leverages shared structural information across multiple seismic surveys to enhance time-lapse inversion quality and provide robust uncertainty quantification. We also present a computationally efficient weak formulation that significantly reduces the number of costly forward operator evaluations required, making the method feasible for practical CCUS applications. Synthetic case study results demonstrate the superior performance of πJRM over the independent inversion method. Specifically, we show that jointly inverting multiple time-lapse surveys greatly improved the accuracy of CO_2 plume reconstructions compared to independent recovery; also, inversion with non-replicated acquisition yields less noise compared to replicated acquisition in a probabilistic setup. Furthermore, collecting more seismic surveys over the same monitoring interval enhances reconstruction performance, reduces uncertainty, and improves repeatability of results. By operating within a probabilistic framework, πJRM also provides essential uncertainty quantification, crucial for reliable risk-averse strategies and informed decision-making in CCUS projects.

ACKNOWLEDGMENTS

This research was carried out with the support of Georgia Research Alliance and partners of the ML4Seismic Center.

During the preparation of this work, the authors used ChatGPT to refine sentence structures and improve the readability of the manuscript. After using this service, the authors reviewed and edited the content as needed and take full responsibility for the content of the publication.

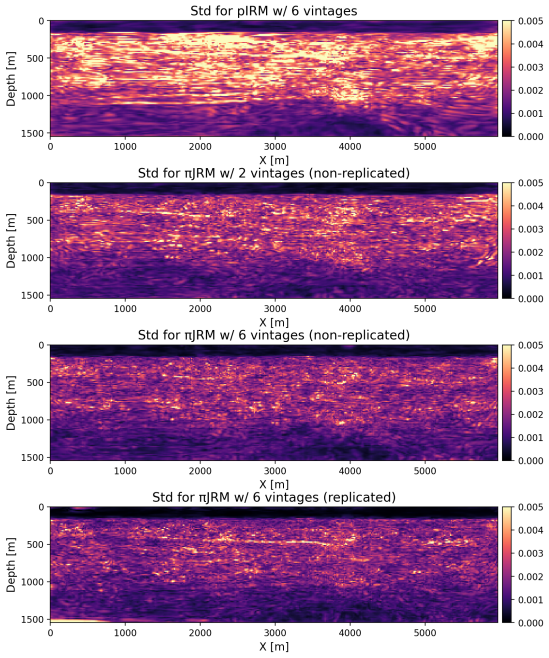

Figure 4: Comparison of uncertainty. From top to bottom: uncertainty of the last vintage after inversion w/ independent method pIRM for $N = 6$ surveys; w/ joint method πJRM and *non-replicated* acquisition for $N = 2$ surveys; w/ πJRM and *non-replicated* acquisition for $N = 6$ surveys; w/ πJRM and *replicated* acquisition for $N = 6$ surveys.

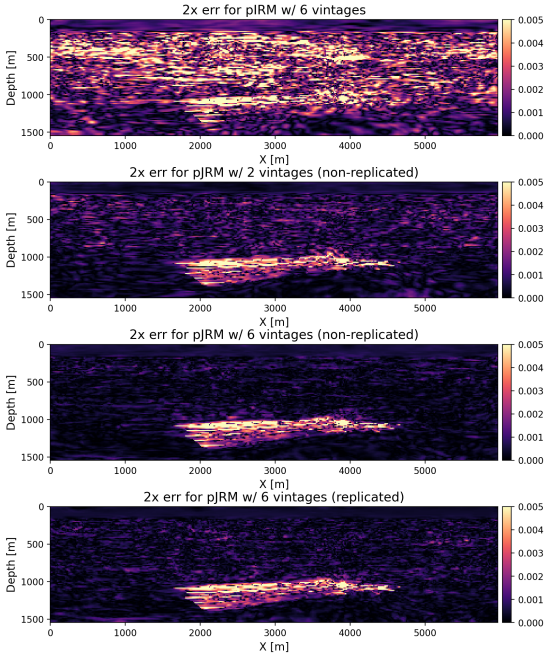

Figure 5: Comparison of error. From top to bottom: $2\times$ error of time-lapse image w/ pIRM for $N = 6$ surveys; w/ πJRM and *non-replicated* acquisition for $N = 2$ surveys; w/ πJRM and *non-replicated* acquisition for $N = 6$ surveys; w/ πJRM and *replicated* acquisition for $N = 6$ surveys.

REFERENCES

Arts, R., O. Eiken, A. Chadwick, P. Zweigel, L. Van der Meer, and B. Zinszner, 2004, Monitoring of co2 injected at sleipner using time-lapse seismic data: Energy, **29**, 1383–1392.

Chadwick, A., and R. Arts, 2010, Monitoring of co_2 injected at sleipner using time-lapse seismic data: Energy Procedia, **1**, 1677–1684.

Gahlot, A. P., M. Louboutin, and F. J. Herrmann, 2023, Time-lapse seismic monitoring of geological carbon storage with the non-linear joint recovery model: Presented at the International Meeting for Applied Geoscience and Energy. ((IMAGE, Houston)).

Heckel, R., and P. Hand, 2019, Deep decoder: Concise image representations from untrained non-convolutional networks.

Leong, O., A. F. Gao, H. Sun, and K. L. Bouman, 2023, Ill-posed image reconstruction without an image prior: CoRR.

Lumley, D., 2001, Time-lapse seismic reservoir monitoring: Geophysics, **66**, 50–53.

Møyner, O., G. Bruer, and Z. Yin, 2023, sintefmath/jutuldarcy.jl: v0.2.3.

Oghenekohwo, F., and F. J. Herrmann, 2015, Compressive time-lapse seismic data processing using shared information: Presented at the CSEG Annual Conference Proceedings. ((CSEG, Calgary)).

Orozco, R., A. Siahkoohi, M. Louboutin, and F. J. Herrmann, 2024, Aspire: Iterative amortized posterior inference for bayesian inverse problems.

Peters, B., and F. J. Herrmann, 2019, Algorithms and software for projections onto intersections of convex and non-convex sets with applications to inverse problems: CoRR, **abs/1902.09699**.

Ringrose, P., 2020, How to store co2 underground: Insights from early-mover ccs projects.

———, 2023, Storage of carbon dioxide in saline aquifers: Building confidence by forecasting and monitoring: Society of Exploration Geophysicists.

Sun, C., A. Malcolm, R. Kumar, and W. Mao, 2024, Enabling uncertainty quantification in a standard full-waveform inversion method using normalizing flows: Geophysics, **89**, R493–R507.

Virieux, J., and S. Operto, 2009, An overview of full-waveform inversion in exploration geophysics: Geophysics, **74**, WCC1–WCC26.

Wilson, M., M. Monea, S. Whittaker, D. White, D. Law, and R. Chalaturnyk, 2004, Iea ghg weyburn co {sub 2} monitoring and storage project: summary report 2000-2004.

Witte, P. A., M. Louboutin, N. Kukreja, F. Luporini, M. Lange, G. J. Gorman, and F. J. Herrmann, 2019, A large-scale framework for symbolic implementations of seismic inversion algorithms in julia: Geophysics, **84**, F57–F71.

Yin, Z., M. Louboutin, and F. J. Herrmann, 2021, Compressive time-lapse seismic monitoring of carbon storage and sequestration with the joint recovery model: SEG International Exposition and Annual Meeting, SEG, D011S145R001.